.

Effect of secondary electron emission on nonlinear dust acoustic wave propagation in a complex plasma with negative equilibrium dust charge

Subrata Bhakta, Uttam Ghosh, and Susmita Sarkar

Citation: Physics of Plasmas **24**, 023704 (2017); doi: 10.1063/1.4976711
View online: http://dx.doi.org/10.1063/1.4976711
View Table of Contents: http://aip.scitation.org/toc/php/24/2
Published by the American Institute of Physics

PHYSICS OF PLASMAS 24, 023704 (2017)

Effect of secondary electron emission on nonlinear dust acoustic wave propagation in a complex plasma with negative equilibrium dust charge

Subrata Bhakta,[1,a)] Uttam Ghosh,[2,b)] and Susmita Sarkar[2,c)]
[1]Department of Mathematics, S. A. Jaipuria College, Kolkata 700005, India
[2]Department of Applied Mathematics, University of Calcutta, Kolkata 700009, India

(Received 24 May 2016; accepted 3 February 2017; published online 21 February 2017)

In this paper, we have investigated the effect of secondary electron emission on nonlinear propagation of dust acoustic waves in a complex plasma where equilibrium dust charge is negative. The primary electrons, secondary electrons, and ions are Boltzmann distributed, and only dust grains are inertial. Electron-neutral and ion-neutral collisions have been neglected with the assumption that electron and ion mean free paths are very large compared to the plasma Debye length. Both adiabatic and nonadiabatic dust charge variations have been separately taken into account. In the case of adiabatic dust charge variation, nonlinear propagation of dust acoustic waves is governed by the KdV (Korteweg-de Vries) equation, whereas for nonadiabatic dust charge variation, it is governed by the KdV-Burger equation. The solution of the KdV equation gives a dust acoustic soliton, whose amplitude and width depend on the secondary electron yield. Similarly, the KdV-Burger equation provides a dust acoustic shock wave. This dust acoustic shock wave may be monotonic or oscillatory in nature depending on the fact that whether it is dissipation dominated or dispersion dominated. Our analysis shows that secondary electron emission increases nonadiabaticity induced dissipation and consequently increases the monotonicity of the dust acoustic shock wave. Such a dust acoustic shock wave may accelerate charge particles and cause bremsstrahlung radiation in space plasmas whose physical process may be affected by secondary electron emission from dust grains. The effect of the secondary electron emission on the stability of the equilibrium points of the KdV-Burger equation has also been investigated. This equation has two equilibrium points. The trivial equilibrium point with zero potential is a saddle and hence unstable in nature. The nontrivial equilibrium point with constant nonzero potential is a stable node up to a critical value of the wave velocity and a stable focus above it. This critical value increases with increasing secondary electron emission. Thus, in the presence of secondary electron emission, higher velocity shock waves are monotonic. The results have been numerically explained considering the presence of Al_2O_3 dust grains in the plasma. *Published by AIP Publishing.*
[http://dx.doi.org/10.1063/1.4976711]

I. INTRODUCTION

Dust grains of different sizes and materials are found everywhere in space where temperature reduces below the melting point. Charging of these dust grains is influenced by several processes, among which secondary electron emission plays a dominant role.[1–3] Several laboratory experiments have been performed to study this secondary electron emission from dust grains.[5] When primary electrons impacting sample surfaces are energetic enough, they interact with the bulk material and loose energy due to many collisions. This consequently excites material electrons. Some of the excited electrons then leave the surface, which are the so-called secondary electrons. Such secondary electrons have typical energies of few eV with Maxwellian-like energy distribution.[1–4] The secondary electron yield is defined as the mean number of emitted secondaries per unit primary electron. The energetic dependence of this secondary electron yield can be described by the Sternglass universal curve.[6] This curve shows a maximum value of the secondary electron yield at few tens of eV and approaches zero value at very low and very high energies. The maximum secondary electron yield and the corresponding maximum energy depend on the sample material.

Escape flux of the secondary electrons represents secondary electron current. The sum of the primary electron current, secondary electron current, and ion current vanishes at three values of potential, out of which two are stable and one is unstable. Between two stable equilibrium states, one is positive and the other is negative.[2,3,7] The secondary electron current flowing out of the dust grains produced by the emitted electrons reduces the negativity of grain charge caused by primary electron current flowing to the dust grains. Consequently, equilibrium dust charge may be negative or positive depending on the magnitude of the secondary electron yield. For the low secondary electron yield, equilibrium dust charge remains negative, whereas for the high secondary electron yield, equilibrium dust charge becomes positive.[7] In this paper, we shall consider only negative equilibrium dust charge, for the study of nonlinear propagation of dust acoustic waves.

a)E-mail: subratabhakta88@gmail.com
b)E-mail: uttam.ghosh.math@gmail.com
c)E-mail: susmita62@yahoo.co.in

Secondary electron emission influences wave propagation characteristics in the dusty plasma. The dusty plasma sustains low frequency dust acoustic and dust ion acoustic waves whose linear and nonlinear theories have been extensively studied by several authors since the last decade of the twentieth century considering both fixed charges and variable charges on dust grains.[8–11] All of these theories were developed considering the dust charging by the flow of plasma current. No secondary emission was taken into account. The effect of secondary electron emission on wave propagation in the dusty plasma was first considered by Gupta *et al.*[12] Its linear theory was investigated considering both negative and positive equilibrium dust charges.[12–14] The effect of secondary electron emission on the growth of Jean's instability in a self gravitating dusty plasma has also studied for both weak and strong secondary electron yields.[15,16] The presence of nonthermal electrons and ions along with secondary electrons has also been considered in further study.[17,18] But nonlinear wave propagation in the presence of secondary electron emission from dust grains in a complex plasma is still unexplored, which is reported first time in this paper.

Charge variation on dust grains may be of both adiabatic and nonadiabatic nature. For adiabatic dust charge variation, dust charging frequency is very high compared to dust plasma frequency, which makes $\frac{\omega_{pd}}{\nu_d}$ zero, where ω_{pd} is the dust plasma frequency and ν_d is the dust charging frequency. Hence, the time scale of dust charging (reciprocal of the dust charging frequency) is very small compared to the time scale of oscillations of dust grains in the plasma, which causes a very fast dust charging. On the other hand, for nonadiabatic dust charge variation, dust charging frequency is small, and hence, charging time is large compared to the adiabatic dust charge variation. Thus, nonadiabatic dust charging process is a slow process. Baisong *et al.*[19] showed that the effect of adiabatic variation of dust charges generates rarefied dust acoustic solitary waves when the Mach number lies within an appropriate regime depending on the system parameters. In the magnetized dusty plasma, such adiabatic charge variation was considered by Shen[20] to show the generation of rarefied dust acoustic solitary waves and studied their instability region under transverse perturbation.

The effect of nonadiabaticity of dust charge variation on dust acoustic solitary waves was first considered by Gupta *et al.*[10] who reported the generation of the dust acoustic shock wave caused by the nonadiabaticity generated dissipative effect. None of the above studies of the effect of adiabatic and nonadiabatic dust charge variations on the dust acoustic solitary wave involved the secondary emission effect. We are first time reporting the effect of secondary electron emission on nonlinear dust acoustic wave propagation in the presence of both adiabatic and nonadiabatic dust charge variations.

In the present paper, equilibrium dust charge has been considered negative. As dust acoustic waves are very low frequency waves, primary electrons, secondary electrons, and ions are considered to follow Boltzmann distribution, only the dust grains under consideration are inertial. Both electron-neutral and ion-neutral collisions have been neglected with the assumption that electron and ion mean free paths are very large compared to the plasma Debye length. Our reductive perturbation analysis shows the existence of the dust acoustic soliton whose amplitude and width both depend on secondary electron yield δ_M. Numerically, it has been seen that this dust acoustic soliton is rarefied, and its amplitude decreases and width increases with increasing secondary electron emission. This is because increasing secondary electron emission increases both coefficients of nonlinearity and dispersion when equilibrium dust charge is negative. Consequently, dust acoustic solitons move slower. Excitation of dust acoustic solitary waves by pulse modulating discharge voltage in an Argon plasma impregnated with kaolin dust particles with negative potential and its propagation was experimentally investigated[21] but any experiment on dust acoustic solitary wave including the effect of secondary electron emission has not been reported yet.

Earlier investigations[10,11] showed that nonadiabaticity in the dust charge variation causes the Burger effect giving rise to the dust acoustic shock wave. This shock wave is dispersion dominated for weak nonadiabaticity and dissipation dominated for strong nonadiabaticity. Our investigation shows that the ratio of the coefficients of the Burger term (dissipation) and the dispersion term increases with increasing secondary electron emission, which implies that secondary emission pronounces the dissipative character in the wave propagation process. Consequently, the dust acoustic shock wave gains monotonicity. Nakamura *et al.*[22] experimentally observed that an ion acoustic oscillatory shock wave in the Ar plasma transforms to the monotonic shock wave when it travels through the dusty plasma column. They integrated the KdV-Burger equation numerically taking experimental parameters into account and compared the results with experimental findings. Observation of the dust acoustic shock waves in the strongly coupled dusty plasma has been recently reported by Sharma *et al.*[23] allowing a supersonic flow of charged microparticles to perturb a stationary dust fluid to excite the dust acoustic shock wave. There has not been reported yet any experiment on the dust acoustic shock wave including the effect of secondary electron emission.

We have also studied the nature of the phase space trajectories near the equilibrium points of the KdV-Burger equation determining the nature of the dust acoustic shock wave near those equilibrium points. By stability analysis, we have obtained a cutoff value of the wave velocity below which the nontrivial equilibrium with constant nonzero potential is a stable node and above which it is a stable focus. The phase space trajectories of the nonlinear system with nonadiabaticity generated dissipation approach the stable node monotonically and the stable focus spirally. Our analysis shows that for stronger secondary emission, this cutoff is higher. Hence, the nontrivial equilibrium point remains a stable node even at higher wave velocity. The trivial equilibrium point is a saddle and hence unstable in nature. This stability analysis of the KdV-Burger equation was previously reported by Gupta *et al.*[10] without considering the effect of secondary emission. So the effect of secondary electron emission on the nonlinear dust acoustic wave propagation in the presence of both adiabatic and nonadiabatic dust charge variations with negative equilibrium dust charge and its effect on the stability property of the dynamical system governed by the KdV-Burger equation is being reported first time in this paper.

II. FORMULATION OF THE PROBLEM

We consider here a dusty plasma whose dust grains are charged by secondary electron emission mechanism due to the impact of energetic electrons with dust grains. In the presence of secondary electron emission, three equilibrium dust charge states exist, out of which two are stable and one is unstable. Moreover, between two stable equilibrium dust charge states, one is negative and the other is positive.[1–3,7] We are interested here with the negative equilibrium dust charge state. Thus, the dusty plasma under our consideration consists of primary electrons, secondary electrons, ions, and negatively charged dust grains and satisfies the quasi-neutrality condition,

$$n_{io} = n_{eo} + n_{so} + z_{d0} n_{d0}, \tag{1}$$

where n_{io}, n_{eo}, n_{so}, and n_{d0} are the equilibrium number densities of ions, primary electrons, secondary electrons, and dust grains, respectively, and z_{d0} is the number of charges on the dust grains in equilibrium. Dust charge is fluctuating and behaves as a dynamical variable.

Since we are studying the nonlinear behavior of dust acoustic waves, both electron and ion inertia should be neglected, and only dust inertia should be taken into account. The basic equations describing the model are

$$\mathrm{n_e} = \mathrm{n_{e0}} \exp\left(\frac{\mathrm{e}\phi}{\mathrm{T_e}}\right), \tag{2}$$

$$\mathrm{n_s} = \mathrm{n_{s0}} \exp\left(\frac{\mathrm{e}\phi}{\mathrm{T_s}}\right), \tag{3}$$

$$\mathrm{n_i} = \mathrm{n_{i0}} \exp\left(-\frac{\mathrm{e}\phi}{\mathrm{T_i}}\right), \tag{4}$$

$$\frac{\partial \mathrm{n_d}}{\partial \mathrm{t}} + \frac{\partial}{\partial \mathrm{x}}(\mathrm{n_d u_d}) = 0, \tag{5}$$

$$\frac{\partial \mathrm{u_d}}{\partial \mathrm{t}} + \mathrm{u_d}\frac{\partial \mathrm{u_d}}{\partial \mathrm{x}} = -\frac{\mathrm{q_d}}{\mathrm{m_d}}\frac{\partial \phi}{\partial \mathrm{x}}, \tag{6}$$

$$\frac{\partial \mathrm{q_d}}{\partial \mathrm{t}} + \mathrm{u_d}\frac{\partial \mathrm{q_d}}{\partial \mathrm{x}} = \mathrm{I_i} + \mathrm{I_e} + \mathrm{I_e^s}, \tag{7}$$

$$\frac{\partial^2 \phi}{\partial \mathrm{x}^2} = -4\pi(\mathrm{q_d n_d} + \mathrm{e n_i} - \mathrm{e n_e} - \mathrm{e n_s}), \tag{8}$$

where T_i, T_e, and T_s are the ion, primary, and secondary electron temperatures and ϕ is the plasma potential, q_d, m_d, u_d, n_d are, respectively, the charge, mass, velocity, and number density of cold dust grains. I_i and I_e are the ion and primary electron current flowing to the dust grains and I_e^s is the secondary electron current flowing out of the dust grains. In the case of negatively charged dust grains, I_i, I_e, and I_e^s take the form,[2]

$$\mathrm{I_i} = \pi \mathrm{r_0}^2 \mathrm{e}\sqrt{\frac{8\mathrm{T_i}}{\pi \mathrm{m_i}}}\mathrm{n_i}\left(1 - \frac{\mathrm{e q_d}}{\mathrm{r_0 T_i}}\right), \tag{9}$$

$$\mathrm{I_e} = -\pi \mathrm{r_0}^2 \mathrm{e}\sqrt{\frac{8\mathrm{T_e}}{\pi \mathrm{m_e}}}\mathrm{n_e} \exp\left(\frac{\mathrm{e q_d}}{\mathrm{r_0 T_e}}\right), \tag{10}$$

$$\mathrm{I_e^s} = 3.7\delta_{\mathrm{M}} \pi \mathrm{r_0}^2 \mathrm{e}\sqrt{\frac{8\mathrm{T_e}}{\pi \mathrm{m_e}}}\mathrm{n_e} \exp\left(\frac{\mathrm{e q_d}}{\mathrm{r_0 T_e}}\right)\mathrm{F_5}\left(\frac{\mathrm{E_M}}{4\mathrm{T_e}}\right). \tag{11}$$

Here, $\mathrm{r_0}$ is the grain radius, $\mathrm{m_i}$ and $\mathrm{m_e}$ are the ion and electron masses, and δ_M is the maximum yield of secondary electrons, which occurs when the impinging electrons have the maximum kinetic energy $\mathrm{E_M}$. The function $\mathrm{F_5}(x)$ is given by[8]

$$\mathrm{F_5(x)} = \mathrm{x}^2 \int_0^\infty \mathrm{u}^5 \exp[-(\mathrm{x u}^2 + \mathrm{u})]\mathrm{du}, \quad \text{where } \mathrm{x} = \frac{\mathrm{E_M}}{4\mathrm{T_e}}. \tag{12}$$

Here, $\mathrm{I_i}$ and $\mathrm{I_e^s}$ both correspond to positive sign as both of them increase the positivity of the dust charge in spite of the fact that $\mathrm{I_i}$ flows towards the dust grain and $\mathrm{I_e^s}$ flows out of the dust grain. On the other hand, the sign of $\mathrm{I_e}$ is negative as it increases the negativity of the grain charge.

III. INVESTIGATION OF SMALL AMPLITUDE STRUCTURES

We shall now use the reductive perturbation technique to study the small amplitude nonlinear structures propagating in a dusty plasma for both adiabatic and nonadiabatic dust charge variations. To proceed, we shall first transform all the field variables and then all the basic equations to dimensionless ones. For this purpose, we first define an effective temperature $\mathrm{T_{eff}}$ from the relation

$$\frac{1}{T_{eff}} = \frac{1}{z_{do} n_{do}}\left(\frac{n_{eo}}{T_e} + \frac{n_{so}}{T_s} + \frac{n_{io}}{T_i}\right), \tag{13}$$

which consequently defines the dusty plasma Debye length $\lambda_D = \left(\frac{\mathrm{T_{eff}}}{4\pi \mathrm{z_{d0} n_{d0} e^2}}\right)^{1/2}$ and dust acoustic speed $c_d = \sqrt{\frac{z_{d0} T_{eff}}{m_d}}$, implying $\mathrm{c_d^2} = \lambda_\mathrm{D}^2 \omega_\mathrm{pd}^2$.

Dimensionless variables are,

$$\mathrm{X} = \mathrm{x}/\lambda_\mathrm{d}; \quad \mathrm{T} = \omega_\mathrm{pd}\mathrm{t}; \quad \mathrm{N_d} = \mathrm{n_d}/\mathrm{n_{d0}}; \quad \mathrm{N_i} = \mathrm{n_i}/\mathrm{n_{i0}};$$
$$\mathrm{N_e} = \mathrm{n_e}/\mathrm{n_{e0}}; \quad \mathrm{N_s} = \mathrm{n_s}/\mathrm{n_{s0}}; \quad \mathrm{V_d} = \mathrm{u_d}/\mathrm{c_d};$$
$$\Phi = \frac{\mathrm{e}\phi}{\mathrm{T_e}}; \quad \mathrm{Q_d} = \mathrm{q_d}/\mathrm{e z_{d0}}, \quad \mathrm{q_{do}} = -\mathrm{z_{do}} \mathrm{e}. \tag{14}$$

Here, $\omega_{pd} = \left(\frac{4\pi \mathrm{n_{d0} z_{d0}^2 e^2}}{\mathrm{m_d}}\right)^{1/2}$ is the dust plasma frequency and $\mathrm{z_{d0}}$ is the number of grain charges in equilibrium.

With these normalizations, (2)–(8) take the following forms:

$$\mathrm{N_e} = \exp(\Phi), \tag{15}$$

$$\mathrm{N_s} = \exp\left(\frac{\Phi}{\sigma_s}\right), \tag{16}$$

$$N_i = \exp\left(-\frac{\Phi}{\sigma_i}\right), \tag{17}$$

$$\frac{\partial N_d}{\partial T} + \frac{\partial}{\partial X}(N_d V_d) = 0, \tag{18}$$

$$\frac{\partial V_d}{\partial T} + V_d\frac{\partial V_d}{\partial X} = -\frac{Q_d}{\alpha_d}\frac{\partial \Phi}{\partial X}, \tag{19}$$

$$\left(\frac{\omega_{pd}}{\nu_d}\right)\left(\frac{\partial Q_d}{\partial T} + V_d\frac{\partial Q_d}{\partial X}\right) = \frac{1}{\nu_d}\left(\frac{\bar{I}_i + \bar{I}_e + \bar{I}_e^s}{z_{do}e}\right), \tag{20}$$

$$\frac{\partial^2\Phi}{\partial X^2} = -\frac{1}{\left(1+\frac{\delta_i}{\sigma_i}+\frac{\delta_s}{\sigma_s}\right)}\left(\delta_i \exp\left(-\frac{\Phi}{\sigma_i}\right) - \exp(\Phi) + \delta_s \exp\left(\frac{\Phi}{\sigma_s}\right) + (\delta_i - \delta_s - 1)Q_d N_d\right), \tag{21}$$

where

$$\bar{I}_i = \pi {r_0}^2 e\sqrt{\frac{8T_i}{\pi m_i}} n_{i0} \exp\left(-\frac{\Phi}{\sigma_i}\right)\left(1 - \frac{zQ_d}{\sigma_i}\right), \tag{22}$$

$$\bar{I}_e = -\pi {r_0}^2 e\sqrt{\frac{8T_e}{\pi m_e}} n_{e0} \exp(\Phi)(zQ_d), \tag{23}$$

$$\bar{I}_e{}^s = 3.7\delta_M \pi {r_0}^2 e\sqrt{\frac{8T_e}{\pi m_e}} n_{e0} \exp(\Phi + zQ_d) F_5\left(\frac{E_M}{4T_e}\right), \tag{24a}$$

with

$$\alpha_d = \frac{\delta_i - \delta_s - 1}{\frac{\delta_i}{\sigma_i} + \frac{\delta_s}{\sigma_s} + 1}, \quad \delta_i = \frac{n_{i0}}{n_{e0}}, \quad \delta_s = \frac{n_{s0}}{n_{e0}},$$
$$\sigma_i = \frac{T_i}{T_e}, \quad \sigma_s = \frac{T_s}{T_e} \quad \text{and} \quad z = z_{d0}e^2/r_0 T_e. \tag{24b}$$

The value of z cannot be taken arbitrary. It should be chosen in a way to maintain the quasi-neutrality condition (1). This follows that δ_i should be greater than 1 when equilibrium dust charge is negative. For this purpose, we need to express δ_i as a function of z, which can be done from the equilibrium current balance equation,

$$\bar{I}_i + \bar{I}_e + \bar{I}_e^s = 0. \tag{25}$$

This gives,

$$\delta_i = \sqrt{\frac{m_i}{m_e}}\frac{\sqrt{\sigma_i}}{\sigma_i + z} e^{-z}\alpha_{1s}, \quad \alpha_{1s} = 1 - 3.7\delta_M F_5\left(\frac{E_M}{4T_e}\right). \tag{26}$$

Thus, z must satisfy the condition,

$$\sqrt{\frac{m_i}{m_e}}\frac{\sqrt{\sigma_i}}{\sigma_i + z} e^{-z}\alpha_{1s} > 1. \tag{27}$$

For the study of small amplitude structures in the dusty plasma in the presence of secondary electron emission with the negative equilibrium dust charge, we employ the reductive perturbation technique, using the stretched coordinates $\xi = \varepsilon^{1/2}(X - \lambda T)$ and $\tau = \varepsilon^{3/2}T$, where ε is a small parameter and λ is the wave velocity normalized by c_d. The variables N_d, V_d, Φ, and Q_d are then expanded as

$$\begin{aligned} N_d &= 1 + \varepsilon N_{d1} + \varepsilon^2 N_{d2} + \ldots, \\ V_d &= \varepsilon V_{d1} + \varepsilon^2 V_{d2} + \ldots, \\ \Phi &= \varepsilon \Phi_1 + \varepsilon^2 \Phi_2 + \ldots, \\ Q_d &= -1 + \varepsilon Q_{d1} + \varepsilon^2 Q_{d2} + \varepsilon^3 Q_{d3} + \ldots. \end{aligned} \tag{28}$$

Substituting these expansions into Equations (15)–(21) with (22)–(26), we collect the terms of different powers of ε. In the lowest order of ε, we obtain,

$$\lambda N_{d1} = V_{d1}, \quad V_{d1} = -\frac{\Phi_1}{\lambda\alpha_d}, \quad N_{d1} = -\frac{\Phi_1}{\lambda^2\alpha_d},$$
$$\Phi_1 + \alpha_d(N_{d1} - Q_{d1}) = 0. \tag{29}$$

To the next higher order in ε, we have the following set of equations:

$$\frac{\partial N_{d1}}{\partial \tau} - \lambda\frac{\partial N_{d2}}{\partial \xi} + \frac{\partial}{\partial \xi}(N_{d1}V_{d1}) + \frac{\partial V_{d2}}{\partial \xi} = 0, \tag{30}$$

$$\frac{\partial V_{d1}}{\partial \tau} - \lambda\frac{\partial V_{d2}}{\partial \xi} + V_{d1}\frac{\partial V_{d1}}{\partial \xi} = \frac{1}{\alpha_d}\left(\frac{\partial \Phi_2}{\partial \xi} - Q_{d1}\frac{\partial \Phi_1}{\partial \xi}\right), \tag{31}$$

$$\frac{\partial^2 \Phi_1}{\partial \xi^2} = \Phi_2 + \alpha_d N_{d2} - \alpha_d Q_{d2} + \left[\frac{1}{\lambda^2\alpha_d}\left(1 - \frac{1}{\lambda^2}\right) - \frac{1}{2}\frac{\left(\frac{\delta_i}{\sigma_i^2} - \frac{\delta_s}{\sigma_s^2} - 1\right)}{\left(\frac{\delta_i}{\sigma_i} - \frac{\delta_s}{\sigma_s} + 1\right)}\right]\Phi_1^2. \tag{32}$$

The above set of equations is common to both adiabatic and nonadiabatic dust charge variations. But the reductive perturbation in the grain charging equation (20) will be different in these two different cases. We shall now consider Equation (20) separately for adiabatic and nonadiabatic dust charge variations.

A. Adiabatic dust charge variation

In the case of adiabatic dust charge variation, dust grains are charged in fast time scale. Hence, dust charging frequency ν_d is very high compared to the dust plasma frequency. With this approximation, $\frac{\omega_{pd}}{\nu_d} \approx 0$, which reduces (20) to,

$$\bar{I}_i + \bar{I}_e + \bar{I}_e^s = 0. \tag{33}$$

Equating from both sides of the terms containing ε and ε^2, we get Q_{d1} and Q_{d2} in the following form:

$$Q_{d1} = -\beta_d\Phi_1, \quad Q_{d2} = -\beta_d\Phi_2 + \gamma_d\Phi_1^2, \tag{34}$$

where

$$\beta_d = \frac{\beta_b}{z\beta_a}; \quad \beta_a = \sqrt{\frac{m_e^i}{\sigma_i}}\alpha_{1s} + \frac{\delta_i}{\sigma_i};$$
$$\beta_b = \sqrt{\frac{m_e^i}{\sigma_i}}\alpha_{1s}e^{-z} + \frac{\delta_i}{\sigma_i}\left(1 + \frac{z}{\sigma_i}\right), \quad m_e^i = \frac{m_i}{m_e}, \tag{35}$$

and

$$\gamma_d = \frac{\gamma_c}{z_0\beta_a}, \quad \gamma_c = \gamma_{c1} + \gamma_{c2} + \gamma_{c3},$$
$$\gamma_{c1} = 0.5\left[\sqrt{\frac{\delta_i}{\sigma_i^2}}\left(1 + \frac{z}{\sigma_i}\right) - \sqrt{\frac{m_e^i}{\sigma_i}\alpha_{1s}e^{-z}}\right];$$
$$\gamma_{c2} = \left[\sqrt{\frac{m_e^i}{\sigma_i}}\alpha_{1s}(1-z) - \frac{\delta_i}{\sigma_i^2}\right](z\beta_d),$$
$$\gamma_{c3} = \left[-0.5\sqrt{\frac{m_e^i}{\sigma_i}}\alpha_{1s}\right](z\beta_d)^2, \quad \lambda = \frac{1}{\sqrt{1+\alpha_d\beta_d}}. \tag{36}$$

λ being the normalized phase velocity of the dust acoustic wave.

Eliminating all the second-order terms from Equations (30) to (34), we get the KdV equation

$$\frac{\partial\Phi_1}{\partial\tau} + \mathrm{a}\Phi_1\frac{\partial\Phi_1}{\partial\xi} + \mathrm{b}\frac{\partial^3\Phi_1}{\partial\xi^3} = 0, \tag{37}$$

where,

$$\mathrm{a} = \mathrm{b}\left[\frac{\left(\frac{\delta_i}{\sigma_i^2} - \frac{\delta_s}{\sigma_s^2} - 1\right)}{\left(\frac{\delta_i}{\sigma_i} - \frac{\delta_s}{\sigma_s} + 1\right)} + 2\alpha_d\gamma_d - \frac{3}{\lambda^2\alpha_d}\right],$$
$$\mathrm{b} = \frac{\lambda^3}{2} = \frac{1}{2}(1+\alpha_d\beta_d)^{-3/2}. \tag{38}$$

The travelling wave solution of Equation (37) can be written as

$$\Phi_1 = \Phi_{1m}\,\mathrm{sech}^2\left[\frac{(\xi - M\tau)}{w}\right], \tag{39}$$

which represents a soliton with amplitude $\Phi_{1m} = \frac{3M}{a}$ and width $w = 2\sqrt{\frac{b}{M}}$. M is the Mach number. Here, both Φ_{1m} and w depend on the secondary electron yield δ_M through the coefficients a and b, respectively. From the expressions of a and b in (38) and α_d, β_d in (24a) and (35), it is clear that a and b are functions of $\delta_i\left(=\frac{n_{i0}}{n_{e0}}\right)$, which depends on δ_M through α_{1s} by (26). Thus, the change in the secondary electron yield δ_M changes a and b and hence changes the amplitude and width of the soliton.

B. Nonadiabatic dust charge variation

In the case of nonadiabatic dust charge variation, dust grains are charged in comparatively slow time scale so that dust charging frequency ν_d is not very high compared to dust plasma frequency. With this approximation, $\frac{\omega_{pd}}{\nu_d}$ is small but finite. We assume

$$\frac{\omega_{pd}}{\nu_d} = \nu\sqrt{\varepsilon}, \tag{40}$$

where ε is small and ν is of order unity.

The dust charge perturbation is then governed by

$$Q_{d1} = -\beta_d\Phi_1;$$
$$Q_{d2} = -\beta_d\Phi_2 + \gamma_d\Phi_1^2 - \lambda\nu\beta_d\delta_i\left(\frac{1+\sigma_i+z_0}{\sigma_i\beta_a}\right)\frac{\partial\Phi_1}{\partial\xi}, \tag{41}$$

which has been obtained from Equations (20) and (22)–(24) with the perturbation (28) and the nonadiabaticity condition (40).

Eliminating all the second-order terms of Equations (20) and (30)–(32), we get the standard KdV-Burger equation,

$$\frac{\partial\Phi_1}{\partial\tau} + \mathrm{a}\Phi_1\frac{\partial\Phi_1}{\partial\xi} + \mathrm{b}\frac{\partial^3\Phi_1}{\partial\xi^3} = \mu\frac{\partial^2\Phi_1}{\partial\xi^2}, \tag{42}$$

where

$$\mu = \frac{1}{2}\lambda^4\nu\beta_d\left[\frac{\delta_i(1+\sigma_i+z)}{\sigma_i\beta_a}\right] \tag{43}$$

and a and b are the same as in (38).

μ is the coefficient of the Burger term, which is the nonadiabaticity induced dissipation effect and does not exist in the case of adiabatic dust charge variation. In hydrodynamics, viscosity is a dissipative effect due to the friction between moving fluid layers. That effect appears as the forcing term in the right hand side of Navier-Stoke's equation. Nonlinear waves propagating in a viscous medium obey the Burger equation where the Burger term containing the second order space derivative arises due to the effect of the fluid viscosity. If those nonlinear waves propagating in a viscous medium are dispersive, they obey the KdV-Burger equation. But in our present problem, we have not considered any viscous force in the equation of motion of dust grains. So the Burger term here is not due to viscosity but has been generated due to nonadiabaticity of the grain charge variation. As in the nonadiabatic process, dust grains are charged in a slow time scale, such viscous-like dissipation comes into the picture, which cannot be observed, if dust grains are charged in fast time scale following the adiabatic process. Moreover, a, b, and μ are all functions of the secondary electron yield δ_M, so they vary with the change in the secondary electron emission. The KdV-Burger equation (42) possesses the shock solution, which in this problem is a dust acoustic shock. This dust acoustic shock is oscillatory if it is dispersion dominated, and monotonic, if it is dissipation dominated depending upon the strength of the secondary electron emission. This emission process influences the acceleration of charge particles and Bremsstrahlung radiation in the plasma generated by the nonadiabaticity induced dust acoustic shock waves.

IV. STABILITY ANALYSIS

To study the nature of the shock, we shall investigate the stability of the equilibrium points of KdV-Burger equation (42). On transforming to the wave frame $\eta = V\tau - \xi$, where V is the wave velocity, this equation reduces to the ordinary differential equation,

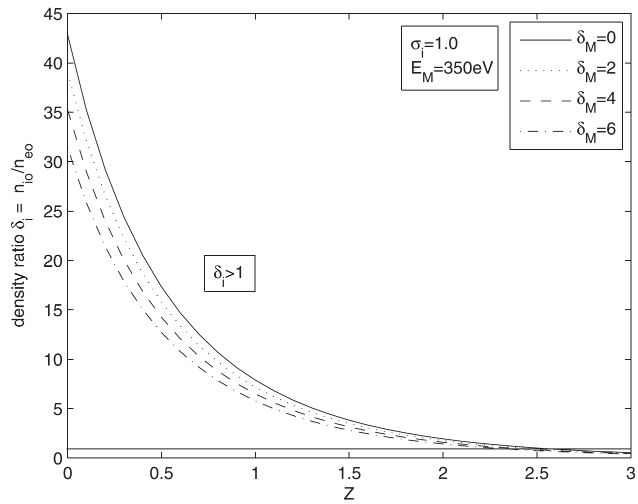

FIG. 1. Plot of $\delta_i (= \frac{n_{i0}}{n_{e0}})$ versus Z $(= \frac{z_{do} e^2}{r_0 T_e})$ for equilibrium dust charge negative.

$$b \frac{d^2 \Phi_1}{d\eta^2} + \mu \frac{d\Phi_1}{d\eta} + \left[\frac{a{\Phi_1}^2}{2} - V\Phi_1 \right] = 0, \tag{44}$$

which has two fixed points $(\Phi_1 = 0, \frac{d\Phi_1}{d\eta} = 0)$ and $(\Phi_1 = \frac{2V}{a}, \frac{d\Phi_1}{d\eta} = 0)$.

The first one $(\Phi_1 = 0, \frac{d\Phi_1}{d\eta} = 0)$ with zero potential is a saddle point and hence unstable in nature. The second one $(\Phi_1 = \frac{2V}{a}, \frac{d\Phi_1}{d\eta} = 0)$ with nonzero potential is a stable node if $\frac{\mu^2}{4b} > V$ and a stable focus if $\frac{\mu^2}{4b} < V$. Thus, for $\frac{\mu^2}{4b} > V$, the dust acoustic shock wave near this equilibrium point is monotonic, whereas it is oscillatory for $\frac{\mu^2}{4b} < V$.

V. NUMERICAL ESTIMATION

For numerical estimation, we have considered[2,6,7] $E_M = 350\,\text{eV}$, $\kappa T_e \approx 20\,\text{eV}$, $\kappa T_s \approx 3\,\text{eV}$, $\delta_s = 0.1$, and Al_2O_3 dust for which δ_M lies in the range of 2–9. Here, $E_M/T_s = 117$, which falls in the range of 100–1300 as mentioned by Meyer-Vernet.[2] Goertz[7] proposed δ_M ranging from 0.5 to 30, E_M ranges from 100 eV to 2000 eV, and the emitted electrons have Maxwellian distribution with T_s ranging from 1 eV to 5 eV. Thus, our assumption $E_M \approx 350\text{eV}$ and $T_s \approx 3\,\text{eV}$ falls in the range prescribed by Goertz.[7] With these numerical data, Figure 1 is plotted for $\delta_i (= \frac{n_{i0}}{n_{e0}})$ versus $z (= \frac{z_{d0} e^2}{r_0 T_e})$ to fix the range of z satisfying the inequality (27). The quasi-neutrality condition (1) follows that the ratio $\frac{n_{i0}}{n_{e0}}$ must be greater than one when equilibrium dust charge is negative. Figure 1 shows that range of z is $0 < z \leq 2.4$. So, the rest of the graphs have been plotted in the range $0.2 < z < 1$ for $\delta_M = 2, 4, 6$. Only Figures 8 and 9 are plotted for $0.2 < z < 0.25$ for clarity of the pictures. The graphs corresponding to $\delta_M = 0$ means there is no secondary electron emission in the grain charging process. Variation of E_M has been neglected since from expressions (11) and (12) secondary electron current vanishes with the increase in E_M. The effect of decrease in E_M has not been investigated here because we have taken $E_M \approx 350\,\text{eV}$ in our numerical calculation, which is the lowermost value of the range 350 eV–1300 eV for Al_2O_3 as mentioned by Meyer-Vernet.[2]

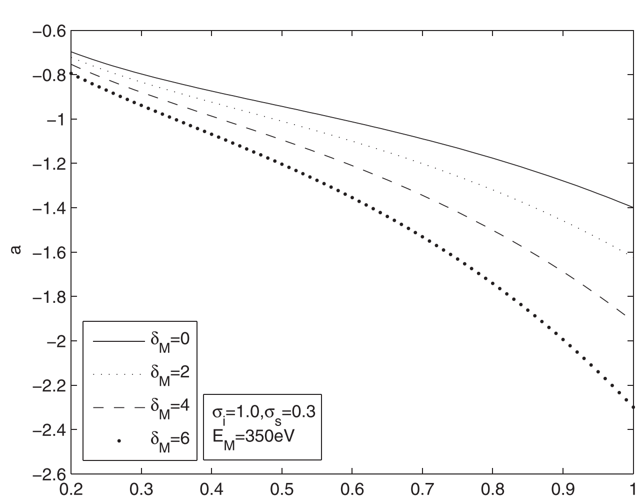

FIG. 2. Plot of the coefficient of nonlinearity a versus z for different δ_M.

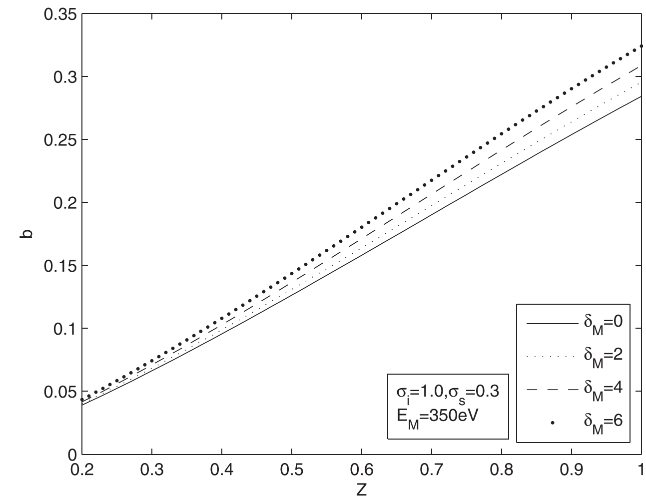

FIG. 3. Plot of the coefficient of the dispersion term b versus z for different δ_M.

Figures 2, 3, and 4 are plotted for the coefficients of nonlinearity "a," dispersion "b," and dissipation "μ," respectively. Figure 2 shows that the coefficient of nonlinearity "a"

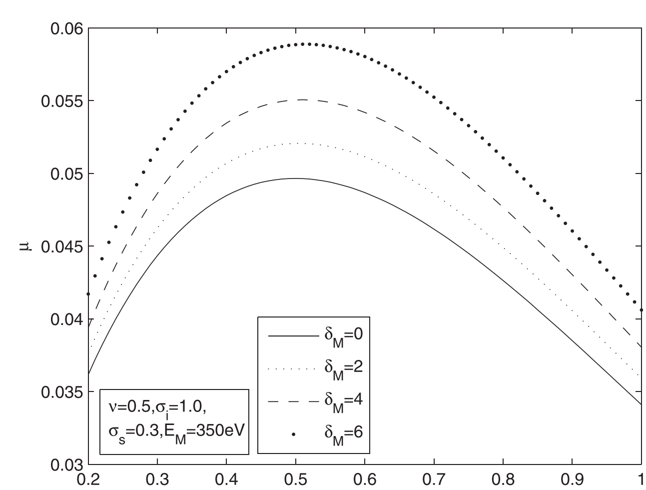

FIG. 4. Plot of the coefficient of the Burgers term μ versus z for different δ_M at $\nu = 0.5$ in the case of nonadiabatic dust charge variation.

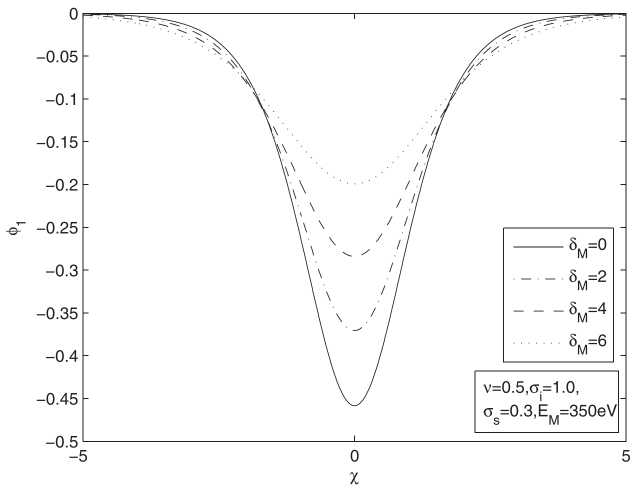

FIG. 5. Plot of the rarefied dust acoustic soliton for different δ_M in the case of adiabatic dust charge variation.

is negative and increases in magnitude with increase in z, i.e., increase in the grain charge number. Figure 3 shows that the coefficient of dispersion "b" increases with an increase in z and Figure 4 shows that the coefficient of Burger term "μ" first increases with z and then decreases after z = 0.5. These three figures show that all these three coefficients increase with increasing secondary electron emission. Thus, increasing secondary electron emission pronounces nonlinearity, dispersion, and dissipation effects when equilibrium dust charge is negative.

The amplitude and width of the dust acoustic soliton for adiabatic dust charge variation are plotted in Figures 6 and 7, respectively. Figure 6 shows the existence of rarefied dust acoustic soliton as its amplitude is negative. Moreover, the amplitude decreases with increasing grain charge number. On the other hand, Figure 7 shows that the width of this rarified dust acoustic soliton increases with increasing grain charge number. These two figures also show that the amplitude of the dust acoustic soliton decreases and width increases with increasing secondary electron emission, which is also clear from Figure 5 representing the profile of

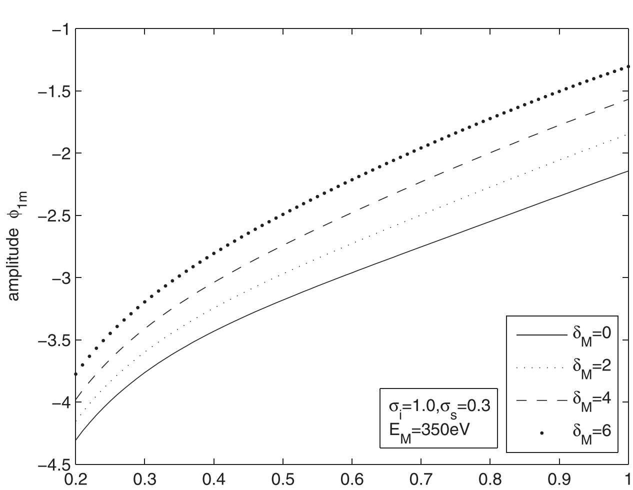

FIG. 6. Plot of the amplitude ϕ_{1m} of the rarefied dust acoustic soliton versus z for different δ_M in the case of adiabatic dust charge variation.

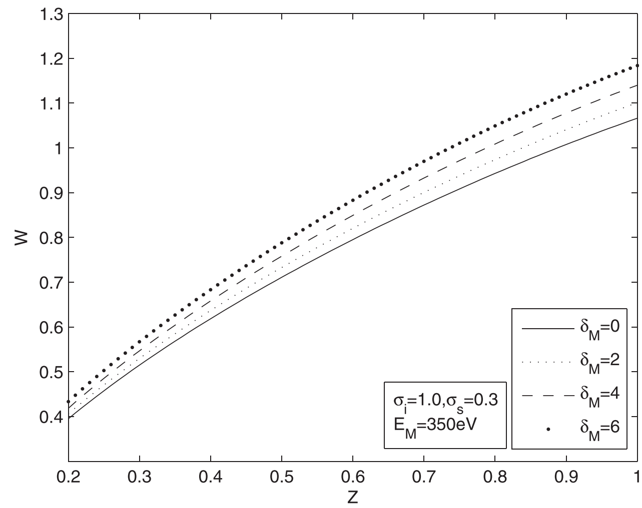

FIG. 7. Plot of the width w of the rarefied dust acoustic soliton versus z for different δ_M in the case of adiabatic dust charge variation.

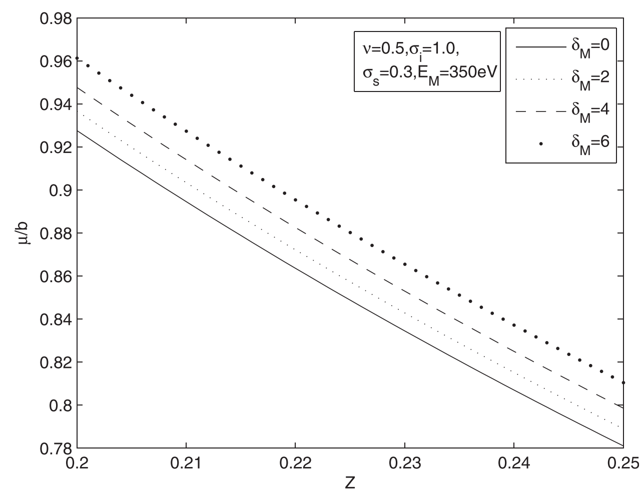

FIG. 8. Plot of the ratio μ/b versus z for different δ_M at $\nu = 0.5$ in the case of nonadiabatic dust charge variation.

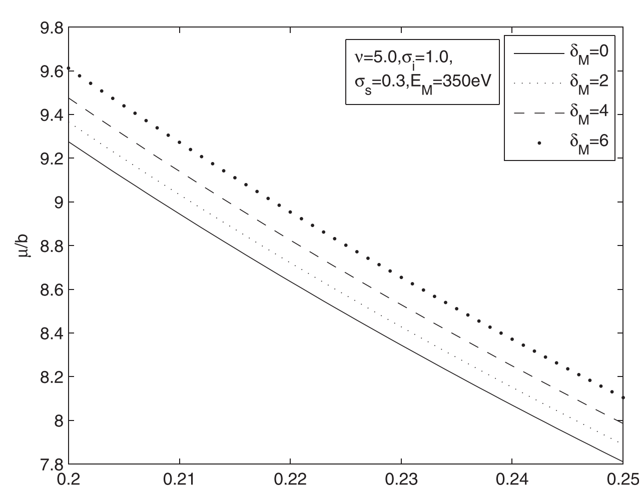

FIG. 9. Plot of the ratio μ/b versus z for different δ_M at $\nu = 5$ in the case of nonadiabatic dust charge variation.

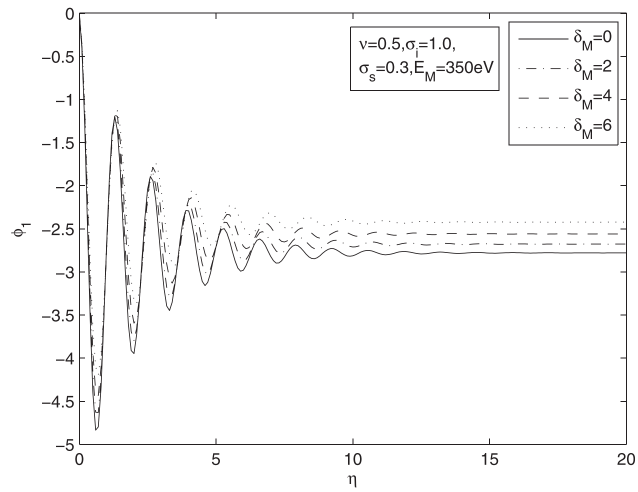

FIG. 10. Oscillatory shock wave for different values of δ_M at $\nu = 0.5$ in the case of nonadiabatic dust charge variation.

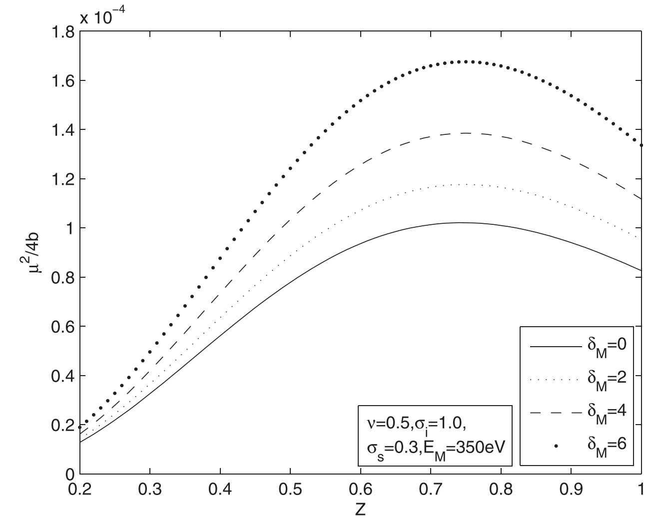

FIG. 12. Plot of the cutoff $\mu^2/4b$ versus z for different δ_M at $\nu = 0.5$ in the case of nonadiabatic dust charge variation.

the dust acoustic soliton. Thus, the dust acoustic soliton moves slower when dust grains are charged by the secondary electron emission process.

In Figures 8 and 9, we have plotted the ratio $\frac{\mu}{b}$ for $\nu = 0.5$ (weak nonadiabaticity) and $\nu = 5$ (strong nonadiabaticity), respectively. Figure 8 shows that at $\nu = 0.5$, this ratio is less than one at all values of z for $\delta_M = 2$, 4, and 6. This means that the dust acoustic shock is dispersion dominated and hence oscillatory for all z at these three values of δ_M. Figure 9 shows that for $\nu = 5$, this ratio $\frac{\mu}{b}$ is greater than one for all z and for all δ_M, i.e., the dust acoustic shock in this case is dissipation dominated and hence monotonic in nature. Both figures show that this ratio $\frac{\mu}{b}$ decreases with increasing grain charge number but increases with increasing secondary electron emission. This implies that the higher grain charge number causes a stronger dispersion effect, whereas higher secondary electron emission pronounces the nonadiabaticity induced dissipation effect, which consequently pronounces the monotonicity of the dust acoustic shock wave. Figure 10 shows the oscillatory nature of the dust acoustic shock for $\nu = 0.5$, M = 1.1, and $\delta_M = 2,4,6$, which becomes monotonic at $\nu = 5$ as shown in Figure 11.[24,25] Both figures show that the magnitude of the potential diminishes with increasing secondary electron emission. Figure 12 plots the cutoff value $\frac{\mu^2}{4b}$ of wave velocity V, below which the dust acoustic shock wave is monotonic near the equilibrium point $\left(\Phi_1 = \frac{2V}{\mathrm{a}}, \frac{d\Phi_1}{d\eta} = 0\right)$ of the KdV-Burger equation reduced to the nonlinear ordinary differential equation (44).

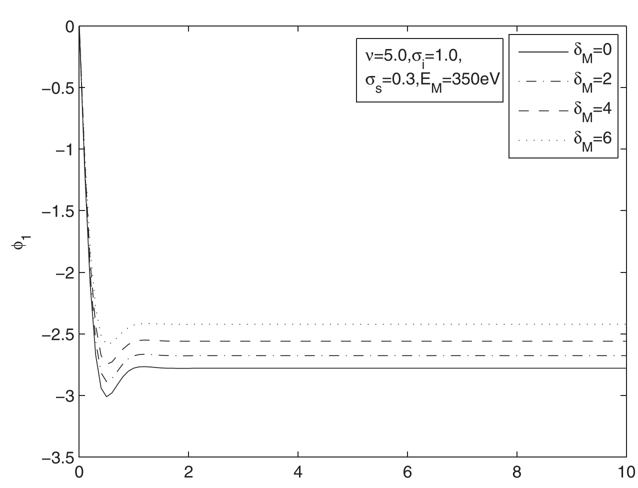

FIG. 11. Monotonic shock wave for different values of δ_M at $\nu = 5$ in the case of nonadiabatic dust charge variation.

This cutoff increases with increasing secondary electron emission, which implies that in the presence of secondary emission higher velocity shock waves are monotonic. Thus, an increase in secondary emission increases the monotonicity of the dust acoustic shock waves when equilibrium dust charge is negative.

VI. CONCLUSION

In this paper, we have studied nonlinear evolution of dust acoustic waves in a complex plasma in the presence of secondary electron emission with negative equilibrium dust charge. The reductive perturbation technique has been used for this analysis. The effect of both electron-neutral and ion–neutral collisions has been neglected. The orbit motion limited (OML) theory has been used to calculate the expressions of primary electron, ion, and secondary electron fluxes over the dust surface. Both the adiabatic and nonadiabatic dust charge variations have been considered. For adiabatic dust charge variation, dust charging frequency is very high compared to the dust plasma frequency, which reduces the ratio of the dust plasma frequency to the dust charging frequency zero value. In this fast grain charging process, nonlinear analysis of the basic equations using the reductive perturbation method gives rise to the KdV equation, which has a soliton solution. In our problem, it is the dust acoustic soliton. Numerical estimation shows that this dust acoustic soliton is rarefied as the coefficient of nonlinearity possesses a negative numerical value. Numerical estimation also shows that the magnitude of the coefficients of nonlinearity and dispersion both increase with increasing grain charge number as well as with increasing secondary electron emission from dust grains. As we know, soliton amplitude is inversely proportional to the coefficient of nonlinearity and soliton width is directly proportional to the coefficient of dispersion; in the case of our problem, amplitude of the dust acoustic soliton should decrease and its width should increase with increasing grain charge number and increasing secondary electron emission. We have justified these by Figures 6, 7, and 5, respectively. Thus, stronger secondary electron emission produces slowly moving dust acoustic solitons as smaller and wider solitons move slowly than taller and sharper solitons.

On the other hand, for nonadiabatic dust charge variation, dust charging frequency is smaller than that of the adiabatic case. Thus, the ratio of the dust plasma frequency to the dust charging frequency in this case is small but a finite number. So, it is a slow grain charging process. In this process, reductive perturbation analysis shows that nonlinear evolution of the dust acoustic wave is governed by the KdV-Burger equation, which possesses the dust acoustic shock solution. This Burger term arises solely due to the nonadiabaticity of dust charge variation. The dust acoustic shock wave is monotonic if it is dissipation dominated, and oscillatory, if it is dispersion dominated. Our numerical estimation shows that secondary electron emission from dust grains increases the magnitude of the dissipation-dispersion ratio and pronounces the monotonicity of the dust acoustic shock waves. The amplitude of both the oscillatory and monotonic shock waves diminishes with increasing secondary electron emission. Finally, we can conclude that in the presence of negatively charged dust grains, strong secondary electron emission reduces the amplitude of both the dust acoustic soliton and the dust acoustic shock wave. Hence, grain charging by the secondary electron emission process is not favorable for nonlinear propagation of dust acoustic waves when equilibrium dust charge is negative. Nonadiabaticity induced shock waves may be responsible for many important physical phenomena in space plasmas. It may accelerate the charge particles and cause bremsstrahlung radiation. Increasing secondary electron emission may slower this acceleration process as it reduces the amplitude of dust acoustic shock when equilibrium grain charge is negative.

ACKNOWLEDGMENTS

Authors wish to acknowledge University Grants Commission for providing financial support through the Special Assistance Program (SAP).

[1]E. C. Whipple, Rep. Prog. Phys. **44**, 1197 (1981).
[2]N. Meyer-Vernet, Astron Astrophys. **105**, 98 (1982).
[3]M. Horanyi, Ann. Rev. Astrophys. **34**, 383 (1996).
[4]O. Hachenberg and W. Brauer, Adv. Electron. Electron Phys. **11**, 413 (1959).
[5]H. Bruining, *Physics and Application of Secondary Electron Emission* (McGraw-Hill Book Co., Inc., 1954).
[6]E. Sternglass, Scientific Paper No. 6-94410-2-P9, Westinghouse Research Laboratories, Pittsburgh, 1957.
[7]C. K. Goertz, Rev. Geophys. **27**(2), 271, doi:10.1029/RG027i002p00271 (1989).
[8]P. K. Shukla and A. A. Mamun, *Introduction to Physics of Dusty Plasma* (Institute of Physics Publishing/CRC Press, Bristol/Philadelphia, 2001).
[9]F. Verheest, *Waves in Dusty Space Plasmas* (Kluwer Academic Publishers, London, 2000).
[10]M. R. Gupta, S. Sarkar, S. Ghosh, M. Debnath, and M. Khan, Phys. Rev. E **63**, 046406 (2001).
[11]S. Ghosh, S. Sarkar, M. Khan, M. R. Gupta, and K. Avinash, Phys. Lett. A **298**, 49 (2002).
[12]M. R. Gupta, S. Sarkar, B. Roy, A. Karmakar, and M. Khan, Phys. Plasmas **11**, 1850 (2004).
[13]M. R. Gupta, S. Sarkar, B. Roy, A. Karmakar, and M. Khan, Phys. Scr. **71**, 298 (2005).
[14]B. Roy, S. Sarkar, M. Khan, and M. R. Gupta, Phys. Lett. A **364**, 291–296 (2007).
[15]S. Sarkar, B. Roy, S. Maity, M. Khan, and M. R. Gupta, Phys. Plasmas **14**, 042106 (2007).
[16]S. Sarkar, S. Maity, B. Roy, and M. Khan, Phys. Scr. **81**, 025504 (2010).
[17]S. Sarkar, S. Maity, and S. Banerjee, Phys. Scr. **84**, 045501 (2011).
[18]S. Sarkar and S. Bhakta, J. Mod. Phys. **7**, 74 (2016).
[19]X. Baisong, H. Kaifen, and H. Zuquia, Phys. Lett. A **247**, 403 (1998).
[20]D. W. Shen, Chin. Phys. **13**, 598 (2004).
[21]P. Bandyopadhyay, G. Prasad, A. Sen, and P. K. Kaw, Phys. Rev. Lett. **101**, 065006 (2008).
[22]Y. Nakamura, H. Bailung, and P. K. Shukla, Phys. Rev. Lett. **83**, 1602 (1999).
[23]S. K. Sharma, A. Boruah, Y. Nakamura, and H. Bailung, Phys Plasmas **23**, 053702 (2016).
[24]H. R. Pakzad and K. Javidan, Pramana J. Phys. **73**(5), 913 (2009).
[25]S. Mahmood and H. Ur-Rehman, Phys. Plasmas **17**, 072305 (2010).